

addition of alkaline aqueous solutions of the following salts: K_3PO_4 , KOH , K_2HPO_4 , NaOH , K_2CO_3 , and Na_2HPO_4 .

Although several studies^{19–21} have been devoted to the evaluation of the salt influence through the formation of ABSs, a systematic and comprehensive analysis on the salting-out ability of the cations and anions that constitute the salts is still missing. Moreover, most of the authors^{19–21} stated that the Hofmeister series²² is always obeyed. This series was first introduced in 1888 by Franz Hofmeister while describing the ability of ions to precipitate proteins.²² Over the years, there have been numerous aqueous phenomena that have been found to follow the Hofmeister series.²³ There are two main groups that make up this series, well hydrated ions (salting-out species) and poorly hydrated ions (salting-in species). In this context, the phase behavior of ABSs composed of ionic liquids and conventional electrolytes have been explained based on the Gibbs free energy of hydration of the salt ions.^{19–21} However, in previous works using hydrophobic ionic liquids, we have shown that their salting-out by inorganic salts from aqueous media is driven by an entropic process resulting from the preferential formation of water–ion complexes.^{24–26} Therefore, aiming at exploring such a possibility for hydrophilic ionic liquids usually involved in the formation of ABSs, and to gather a broader picture on the molecular mechanisms that govern the formation of these two-phase systems, a broad range of salts was investigated here. The ability of the salts (or salt ions) to induce the formation of ionic-liquid-based ABSs was evaluated by means of the determination of the corresponding ternary phase diagrams at 298 K and atmospheric pressure.

To carry out a study with the widest possible range of salts, the choice of an adequate ionic liquid is a crucial requirement. According to our previous studies the most adequate choice is 1-butyl-3-methylimidazolium trifluoromethanesulfonate, a hydrophilic ionic liquid yet with an improved ability for being salted-out even by carbohydrates²⁷ or amino acids.¹⁵ Although tetrafluoroborate-based ionic liquids are also good candidates capable of easily undergoing liquid–liquid demixing in the presence of aqueous solutions of salts, these ionic liquids are not water-stable and tend to form hydrofluoric acid in aqueous environments.²⁸

EXPERIMENTAL SECTION

Materials. The ionic liquid used in this work was 1-butyl-3-methylimidazolium trifluoromethanesulfonate (or 1-butyl-3-methylimidazolium triflate), $[\text{C}_4\text{mim}][\text{CF}_3\text{SO}_3]$, with a stated purity of >99 wt % and supplied by Iolitec. After drying the ionic liquid under vacuum, at 323 K for a minimum of 48 h, the purity of the ionic liquid was further confirmed by ^1H , ^{13}C , and ^{19}F NMR spectra. The salts used were NaCl > 99.9 wt % from Prolabo, NaCH_3CO_2 > 99.8 wt % and KCl > 99 wt %, both from Pronolab, NaOH > 98.0 wt % from Akzonoble, Na_2SO_4 > 99.0 wt % from Labsolve, Na_2CO_3 > 99.7 wt % from Carlo Erba, $\text{NiCl}_2 \cdot 6\text{H}_2\text{O}$ > 97 wt % from BDH Reagents, NaHCO_3 > 99.5 wt %, $\text{Na}_3\text{C}_6\text{H}_5\text{O}_7 \cdot 2\text{H}_2\text{O}$ > 98 wt %, and $\text{SrCl}_2 \cdot 2\text{H}_2\text{O}$ > 99.0 wt %, all from Merck, $\text{KNaC}_4\text{H}_4\text{O}_6 \cdot 4\text{H}_2\text{O}$ > 99 wt %, NaH_2PO_4 > 99 wt %, Na_2SO_3 > 98 wt %, $\text{MgCl}_2 \cdot 6\text{H}_2\text{O}$ > 99 wt %, $\text{NaHSO}_4 \cdot \text{H}_2\text{O}$ > 97.0 wt %, and CsCl > 99.5 wt %, all from Panreac, and $\text{Na}_3\text{PO}_4 \cdot 12\text{H}_2\text{O}$ > 98 wt %, $\text{CaCl}_2 \cdot 2\text{H}_2\text{O}$ > 99 wt %, Na_2HPO_4 > 99 wt %, $\text{Mg}(\text{CH}_3\text{CO}_2)_2 \cdot 4\text{H}_2\text{O}$ > 99.5 wt %, $\text{Ca}(\text{CH}_3\text{CO}_2)_2 \cdot \text{H}_2\text{O}$ > 99 wt %, and KCH_3CO_2 > 99 wt %, all from Riedel-de-Haën. Small samples (~5 g) of all salts were dried in an air oven at 378 K and for a minimum of 24 h before the preparation of their aqueous solutions for the determination

of the phase diagrams. Double-distilled water, passed through a reverse osmosis system and further treated with Milli-Q plus 185 water purification equipment, was used in all experiments.

Phase Diagrams, Tie-Lines, and Tie-Line Length Measurements. Aqueous solutions of each salt with variable mass fractions (usually close to yet below the saturation solubility in water at room temperature) and aqueous solutions of $[\text{C}_4\text{mim}][\text{CF}_3\text{SO}_3]$ in a range between 70 and 95 wt % were prepared and used for the determination of the corresponding binodal curves. The binodal curves were established at 298 K (± 1 K) and at atmospheric pressure through the cloud point titration method.^{15–17} Repetitive dropwise addition of the aqueous salt solution to the ionic liquid aqueous solution was carried out until the detection of a cloudy solution, that is, the biphasic region, followed by the dropwise addition of water until the formation of a clear and limpid solution, that is, the monophasic region. To complete the phase diagrams, the opposite addition of the ionic liquid aqueous solution to the salt solutions was also carried out. Dropwise additions were carried out under constant stirring. The ternary systems' compositions were determined by weight quantification of all components within $\pm 10^{-4}$ g.

The experimental binodal curves were correlated according to the following equation proposed by Merchuck et al.²⁹

$$[\text{IL}] = A \exp[(B \times [\text{salt}]^{0.5}) - (C \times [\text{salt}]^3)] \quad (1)$$

where $[\text{IL}]$ and $[\text{salt}]$ are the ionic liquid and the salt mass fraction percentages and A , B , and C are constants obtained by the regression of the experimental binodal data.

The tie-lines (TLs) were determined by a gravimetric method originally presented by Merchuck et al.²⁹ for polymer-based ABSs and applied later to ionic-liquid-based ABSs by Rogers and co-workers.⁵ For the determination of each TL, a ternary mixture was prepared by mixing water, ionic liquid, and salt with specified concentrations within the biphasic region and vigorously agitating. The mixtures were then allowed to equilibrate for ~24 h at (298 ± 1) K. After that period, the top and bottom phases were carefully separated and individually weighed within $\pm 10^{-4}$ g. The TLs were determined by a mass balance using the relationship between the weight of the ionic-liquid-rich phase and the composition of the overall system, as detailed elsewhere.^{11,27} The tie-line lengths (TLLs) correspond to the distance between the point in the binodal curve at the bottom phase composition and that at the top phase.^{11,27}

RESULTS AND DISCUSSION

Phase Diagrams. The ability of a large series of organic and inorganic salts to induce the formation of $[\text{C}_4\text{mim}][\text{CF}_3\text{SO}_3]$ -based ABSs was studied at a constant temperature (298 K) and at atmospheric pressure. All of the investigated salts were able to promote ABSs in the presence of concentrated aqueous solutions of $[\text{C}_4\text{mim}][\text{CF}_3\text{SO}_3]$, namely, KCl , CsCl , NaCl , NaCH_3CO_2 , NaOH , NaHCO_3 , NaHSO_4 , NaH_2PO_4 , Na_2HPO_4 , Na_2SO_4 , Na_2CO_3 , Na_2SO_3 , $\text{KNaC}_4\text{H}_4\text{O}_6$, $\text{Na}_3\text{C}_6\text{H}_5\text{O}_7$, Na_3PO_4 , SrCl_2 , MgCl_2 , CaCl_2 , NiCl_2 , $\text{Mg}(\text{CH}_3\text{CO}_2)_2$, $\text{Ca}(\text{CH}_3\text{CO}_2)_2$, and KCH_3CO_2 .

The experimental weight fraction data of the liquid–liquid biphasic systems measured here are detailed in the Supporting Information. The binodal curves of all systems were correlated with eq 1, and the respective parameters A , B , and C , along with their corresponding standard deviations, are listed in Table 1.

Table 1. Values of the Parameters *A*, *B*, and *C* of Equation 1 (and respective standard deviations, σ , and correlation coefficients, R^2) for the $[\text{C}_4\text{mim}][\text{CF}_3\text{SO}_3] + \text{Salt} + \text{H}_2\text{O}$ Systems at 298 K

R^2	$10^5(C \pm \sigma)$	$B \pm \sigma$	$A \pm \sigma$	salt
0.9962	91.9 \pm 10.0	-0.920 \pm 0.010	116.0 \pm 1.2	Na_3PO_4
0.9914	-6.6 \pm 0.8	-1.000 \pm 0.013	249.8 \pm 6.8	$\text{Na}_3\text{C}_6\text{H}_5\text{O}_7$
0.9947	43.1 \pm 7.3	-0.776 \pm 0.010	113.4 \pm 1.5	Na_2HPO_4
0.9960	-26.6 \pm 6.3	-1.122 \pm 0.012	172.4 \pm 2.9	Na_2CO_3
0.9961	6.5 \pm 3.5	-0.912 \pm 0.012	156.2 \pm 2.8	Na_2SO_4
0.9987	-15.2 \pm 1.8	-1.133 \pm 0.006	218.7 \pm 2.1	Na_2SO_3
0.9910	68.2 \pm 6.1	-0.464 \pm 0.012	102.4 \pm 1.7	$\text{KNaC}_4\text{H}_4\text{O}_6$
0.9986	22.4 \pm 3.2	-1.173 \pm 0.043	1087.9 \pm 112.2	MgCl_2
0.9958	13.3 \pm 3.6	-0.903 \pm 0.103	790.0 \pm 230.8	CaCl_2
0.9976	-4.3 \pm 0.9	-1.458 \pm 0.099	6074.3 \pm 2199.3	SrCl_2
0.9962	7.11 \pm 1.6	-0.888 \pm 0.038	656.0 \pm 68.3	NiCl_2
0.9961	-1.5 \pm 1.0	-0.812 \pm 0.013	244.8 \pm 6.9	$\text{Mg}(\text{CH}_3\text{CO}_2)_2$
0.9976	23.2 \pm 2.9	-0.543 \pm 0.020	158.2 \pm 6.4	$\text{Ca}(\text{CH}_3\text{CO}_2)_2$
0.9976	25.6 \pm 1.3	-0.535 \pm 0.009	174.2 \pm 2.8	NaCl
0.9950	3.9 \pm 5.8	-0.882 \pm 0.031	248.8 \pm 15.3	NaCH_3CO_2
0.9953	-220.4 \pm 10.0	-1.799 \pm 0.024	355.8 \pm 11.9	NaOH
0.9983	62.0 \pm 5.0	-0.589 \pm 0.011	123.6 \pm 1.9	NaHCO_3
0.9987	20.2 \pm 1.8	-0.447 \pm 0.010	126.6 \pm 2.3	NaHSO_4
0.9917	6.4 \pm 1.2	-0.723 \pm 0.011	158.5 \pm 3.3	NaH_2PO_4
0.9945	-3.2 \pm 0.4	-0.794 \pm 0.014	329.4 \pm 12.3	KCH_3CO_2
0.9994	15.1 \pm 0.4	-0.330 \pm 0.007	140.6 \pm 2.5	KCl
0.9996	1.4 \pm 0.1	-0.289 \pm 0.009	189.4 \pm 6.6	CsCl

From the correlation coefficients obtained, it is safe to admit that eq 1 provides a good description of the experimental data. The experimental results for the TLs, TLLs, and the percentage weight fraction compositions of salt and ionic liquid in the top and bottom phases are presented in Table 2. It should be noted that “[IL]_{IL}” and “[salt]_{IL}” designate the ionic liquid and salt content at the ionic-liquid-rich phase, “[IL]_{salt}” and “[salt]_{salt}” represent the ionic liquid and salt weight fraction percentages in the salt-rich phase, and “[IL]_M” and “[salt]_M” represent the ionic liquid and salt amounts in the initial mixture used for phase separation. Furthermore, α is the ratio between the weight of the ionic-liquid-rich phase and the total weight of the mixture.

The phase diagrams of the various ternary systems investigated are graphically presented in Figures 1–3. To remove the influence of divergences that could result from different molecular weights of the salts, the saturation curves are compared in molality units.^{13,14,16–18} It should be stressed that the amount of water complexed to the commercial salts was removed in the calculations of the molality of salts and added to the water composition of each phase diagram. Figure 1 reports the saturation curves for NaCl , NaCH_3CO_2 , NaOH , NaHCO_3 , NaH_2PO_4 , NaHSO_4 , Na_2SO_4 , Na_2SO_3 , Na_2CO_3 , Na_2HPO_4 , $\text{KNaC}_4\text{H}_4\text{O}_6$, $\text{Na}_3\text{C}_6\text{H}_5\text{O}_7$, and Na_3PO_4 and allows an evaluation of the salt anion effect in the formation of ionic-liquid-based ABSs. The larger the two-phase region, the stronger the salt's ability to induce the ABS formation. From the gathered results, for instance, at a molality of ionic liquid at which it equals the molality of salt in the binodal curve (i.e., $[\text{IL}] = [\text{salt}]$ in molality units), the salting-out ability of the anions follows the order $\text{PO}_4^{3-} > \text{C}_6\text{H}_5\text{O}_7^{3-} > \text{HPO}_4^{2-} \approx \text{CO}_3^{2-} > \text{SO}_4^{2-} \approx \text{SO}_3^{2-} > \text{C}_4\text{H}_4\text{O}_6^{2-} \gg \text{H}_2\text{PO}_4^- > \text{OH}^- > \text{CH}_3\text{COO}^- \approx \text{HSO}_4^- \approx \text{HCO}_3^- > \text{Cl}^-$. The anion that induces the strongest salting-out effect is PO_4^{3-} , as previously observed by us²⁴ and others.¹⁹ Moreover, with the $[\text{C}_4\text{mim}][\text{CF}_3\text{SO}_3]$ ionic liquid, it is possible to create ABSs even with weak salting-

out species, such as NaCl , KCl , and CsCl . One important observation is that the ion charge plays a significant role because trivalent anions present a stronger salting-out ability than the divalent ones, and these are stronger than monovalent anions. In general, the qualitative trend of the anions' ability to induce the salting-out of the ionic liquid closely follows the Hofmeister series.^{22,23,30}

The phase diagrams displayed in Figure 2, with Cl^- as the common salt anion, and in Figure 3, with CH_3CO_2^- as the common ion, allow the study of the ability of the cations of the salts to promote ABSs. The salts investigated for this purpose were NaCl , CsCl , MgCl_2 , CaCl_2 , SrCl_2 , NiCl_2 , KCl , NaCH_3CO_2 , $\text{Mg}(\text{CH}_3\text{CO}_2)_2$, $\text{Ca}(\text{CH}_3\text{CO}_2)_2$, and KCH_3CO_2 . From the collected data, it is observed that the salting-out ability in the two series of salts is identical and follows the order $\text{Mg}^{2+} \approx \text{Ni}^{2+} \approx \text{Sr}^{2+} > \text{Ca}^{2+} \gg \text{Na}^+ > \text{K}^+ > \text{Cs}^+$ for the chloride-based salts and $\text{Mg}^{2+} > \text{Ca}^{2+} > \text{Na}^+ > \text{K}^+$ for the acetate-based salts. As observed before for the anions, the ion charge plays a dominant role. Divalent cations present a stronger salting-out effect than the monovalent ions. The strongest salting-out inducing cation studied is Mg^{2+} , whereas the weakest salting-out inducing cation is Cs^+ . The cation influence in the salting-out of the ionic liquid $[\text{C}_4\text{mim}][\text{CF}_3\text{SO}_3]$ also follows the Hofmeister series.^{22,23,30}

As stated above, the anion and cation ranks obtained closely follow the well-known Hofmeister series^{22,23} and are in agreement with previous results regarding their salting-out ability toward hydrophobic^{24–26} or hydrophilic ionic liquids.^{19–21} While the Hofmeister rank is phenomenologically well-established, the molecular level mechanisms by which ions operate are still elusive and not well understood. The salting-out inducing ions are usually classified as “kosmotropes”, while the salting-in inducing ions are typically referred to as “chaotropes”, based on their supposed ability to “create” or “destroy” the water bulk structure.^{31–33} Recent experimental solubility data, spectroscopic data, and simulation results have

Table 2. Compositions (wt %) for the $[C_4mim][CF_3SO_3]$ + salt + H_2O Systems at 298 K and Respective Values of α and TLL

TLL	α	weight fraction composition/wt %						salt
		[salt] _{IL}	[IL] _{IL}	[salt] _M	[IL] _M	[salt] _{salt}	[IL] _{salt}	
26.24	0.21	2.31	28.36	3.79	23.14	9.48	3.12	Na ₃ PO ₄
23.70	0.18	2.38	27.75	3.45	23.61	8.33	4.81	
87.58	0.08	1.03	90.77	17.41	12.26	18.92	5.04	Na ₃ C ₆ H ₅ O ₇
62.54	0.09	1.68	68.24	13.10	12.36	14.21	6.96	
46.37	0.36	1.34	46.11	6.00	30.31	14.44	1.63	Na ₂ HPO ₄
40.79	0.34	1.50	43.79	4.91	30.30	11.50	4.25	
29.21	0.26	2.24	32.27	5.19	25.27	13.61	5.36	Na ₂ CO ₃
27.00	0.24	2.33	31.18	4.51	25.10	11.43	5.77	
39.72	0.33	2.05	42.38	5.96	29.76	13.81	4.45	Na ₂ SO ₄
31.98	0.30	2.24	39.88	4.48	30.40	9.59	8.76	
32.82	0.29	2.72	33.86	6.92	25.16	16.99	4.31	Na ₂ SO ₃
30.24	0.25	2.88	32.13	5.97	25.17	15.16	4.50	
45.72	0.59	1.05	63.64	4.01	44.97	8.23	18.49	KNaC ₄ H ₄ O ₆
33.78	0.67	1.61	56.64	3.44	45.53	7.09	23.30	
41.86	0.31	7.22	42.74	10.52	30.04	17.74	2.23	MgCl ₂
35.60	0.19	7.81	36.84	9.64	30.29	17.36	2.54	
61.89	0.49	6.93	70.16	12.01	40.43	17.36	9.15	CaCl ₂
38.22	0.50	7.82	59.36	10.57	40.37	13.29	21.53	
70.22	0.10	9.07	77.60	22.22	15.69	23.66	8.91	SrCl ₂
63.92	0.16	9.37	72.48	20.29	20.03	22.40	9.90	
95.91	0.21	4.48	99.60	17.96	25.04	21.55	5.22	NiCl ₂
73.90	0.20	5.34	83.27	15.26	25.11	17.77	10.42	
55.54	0.44	2.72	64.21	8.50	40.47	15.86	10.25	Mg(CH ₃ CO ₂) ₂
44.67	0.44	3.02	59.68	6.81	40.24	11.56	15.83	
69.95	0.43	1.65	78.64	8.93	39.64	14.48	9.89	Ca(CH ₃ CO ₂) ₂
56.62	0.50	2.42	67.68	8.00	39.73	13.50	12.15	
76.77	0.64	2.05	80.82	6.10	49.96	16.95	5.52	NaCl
65.83	0.57	2.41	75.66	8.12	50.13	14.29	10.91	
43.84	0.32	3.44	48.43	7.45	34.80	15.82	6.38	NaCH ₃ CO ₂
37.22	0.33	3.58	46.84	6.43	34.87	12.20	10.64	
62.86	0.66	1.70	70.59	6.52	49.92	15.96	9.36	NaHSO ₄
50.53	0.73	2.41	63.12	5.47	50.02	13.91	13.92	
53.88	0.38	2.18	54.50	9.05	35.00	20.09	3.68	NaH ₂ PO ₄
44.78	0.39	2.38	51.97	7.00	34.94	14.11	8.76	
29.52	0.65	1.87	55.02	3.29	44.87	5.95	25.78	NaHCO ₃
66.68	0.41	3.27	78.53	12.02	40.25	18.12	13.53	KCH ₃ CO ₂
45.68	0.40	4.78	58.22	9.83	40.47	17.28	14.28	
82.12	0.49	2.16	86.48	11.99	46.07	21.57	6.68	KCl
75.23	0.54	2.84	80.38	11.18	47.13	21.14	7.42	
68.28	0.33	11.11	70.93	32.00	30.11	42.21	10.14	CsCl
50.02	0.31	14.41	60.67	29.95	30.04	37.04	16.06	

cast doubts on this paradigm of the change in the bulk water structure as the main phenomenon behind the effect of salts on the molecules' solubility in water (and, in this particular case, of ionic liquids).^{24–26} Evidences previously reported suggest that salting-out inducing ions act through an entropic effect resulting from the formation of hydration complexes that further cause the dehydration of the solute and the increase of the surface tension of the cavity.^{24–26} A close correlation of the solubility data of hydrophobic ionic liquids in salt aqueous solutions with the molar entropy of hydration of the salt ions was also shown to exist.^{24–26}

Various authors have suggested that the salting-out of ionic liquids to form ABSs can be related to the Gibbs free energy of hydration of the salt ions ($\Delta_{\text{hyd}}G$).^{20,21,34} These explanations are in accordance with results on the phase behavior of ABSs composed of polymers.^{35–38} However, as these studies are focused on the Gibbs free energies, a direct discrimination

between the enthalpic and entropic contributions is not provided.^{35–38} In this context, Haynes and co-workers³⁹ proposed a set of equations derived from the Flory–Huggins theory, aiming at gathering a qualitative assessment on the contributions of enthalpy and entropy through the phase separation in ABSs. Ananthapadmanabhan and Goddard⁴⁰ stated that the phenomenon behind the formation of polymer-based ABSs is very similar to the phase separation observed in polymer aqueous solutions upon heating. Rogers and co-workers⁴¹ reported a correlation between the efficiency of a series of cations in inducing the formation of ABSs and their hydration enthalpies and Gibbs energies. In addition, liquid–liquid equilibria of polymer-based ABSs have shown that the increase in entropy is the driving force for the two-phase separation.⁴² In fact, recent studies are converging up to the idea that the formation of polymer-based ABSs is an entropy-driven process.^{42,43} Particularly, calorimetric investigations on

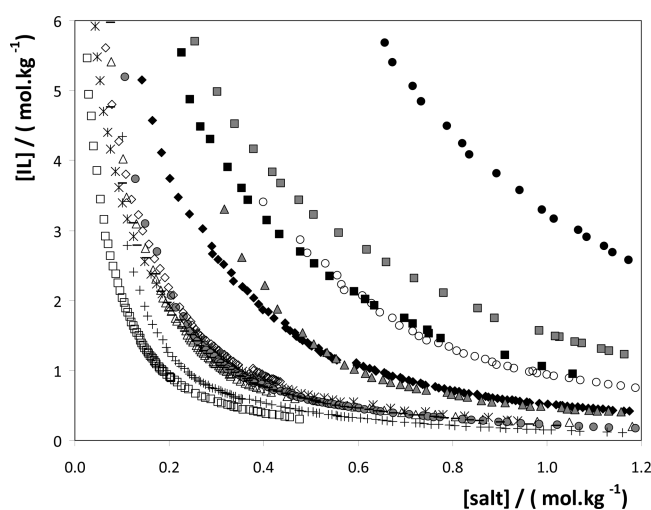


Figure 1. Ternary phase diagrams of the various $[\text{C}_4\text{mim}][\text{CF}_3\text{SO}_3]$ + water + salt systems at 298 K and atmospheric pressure (evaluation of the anion effect): (\square) Na_3PO_4 , (+) $\text{Na}_3\text{C}_6\text{H}_5\text{O}_7$, (*) Na_2HPO_4 , (Δ) Na_2CO_3 , (—) Na_2SO_4 , (gray \bullet) Na_2SO_3 , (\diamond) $\text{KNaC}_4\text{H}_4\text{O}_6$, (\blacklozenge) NaH_2PO_4 , (gray \blacktriangle) NaOH , (\circ) NaCH_3CO_2 , (\blacksquare) NaHSO_4 , (gray \blacksquare) NaHCO_3 , (\bullet) NaCl .

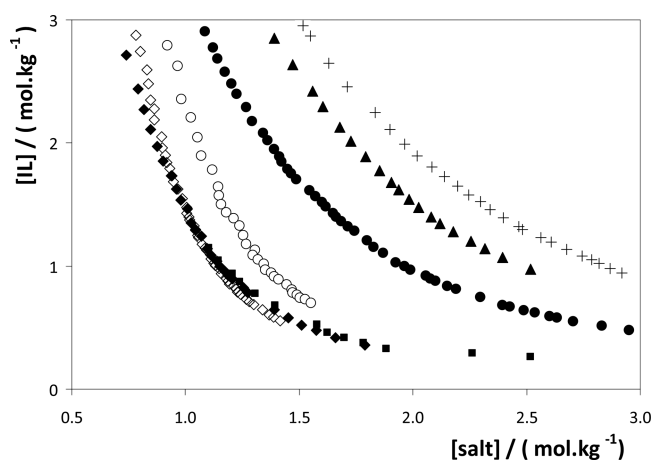


Figure 2. Ternary phase diagrams of the various $[\text{C}_4\text{mim}][\text{CF}_3\text{SO}_3]$ + water + salt systems at 298 K and atmospheric pressure (evaluation of the cation effect for the chloride-based salts): (\diamond) MgCl_2 , (\blacklozenge) NiCl_2 , (\blacksquare) SrCl_2 , (\circ) CaCl_2 , (\bullet) NaCl , (\blacktriangle) KCl , (+) CsCl .

the enthalpies of solution of polymers and electrolytes in aqueous media revealed that the entropy increase is the driving force for the liquid–liquid demixing in ABSs.⁴³

Aiming at testing which is the main mechanism behind the formation of ionic-liquid-based ABSs, as well as to compare the results here obtained with our alternative explanation on the salting-out phenomenon for hydrophobic ionic liquids (which is entropically driven),^{24–26} correlations between the salting-out ability of each salt and the molar Gibbs free energy of hydration or molar entropy of hydration of the ions were attempted. The values of the molar Gibbs free energy of hydration and molar entropy of hydration of the anions and cations studied here are presented in Table 3. The molality of the ionic liquid at which it equals the molality of salt in the binodal curve, hereafter named “saturation solubility”, is adopted as a semiquantitative measure of the ions salting-out strength. The saturation solubilities for the studied systems are reported in Table 3.

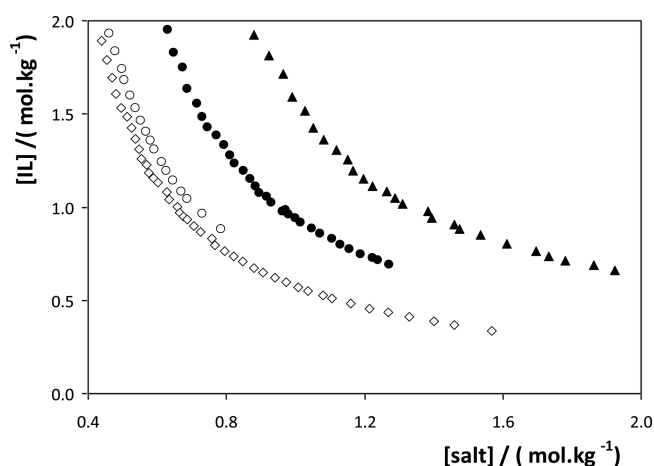


Figure 3. Ternary phase diagrams of the various $[\text{C}_4\text{mim}][\text{CF}_3\text{SO}_3]$ + water + salt systems at 298 K and atmospheric pressure (evaluation of the cation effect for the acetate-based salts): (\diamond) $\text{Mg}(\text{CH}_3\text{CO}_2)_2$, (\circ) $\text{Ca}(\text{CH}_3\text{CO}_2)_2$, (\bullet) NaCH_3CO_2 , (\blacktriangle) KCH_3CO_2 .

Table 3. Molar Entropy of Hydration ($\Delta_{\text{hyd}}S$) and Gibbs Free Energy of Hydration ($\Delta_{\text{hyd}}G$) for the Cations and Anions Investigated^{44–46} and Ionic Liquid Molality at the Saturation Solubility

$\Delta_{\text{hyd}}G/$ ($\text{kJ}\cdot\text{mol}^{-1}$)	$\Delta_{\text{hyd}}S/$ ($\text{J}\cdot\text{K}^{-1}\cdot\text{mol}^{-1}$)	$([\text{IL}] = [\text{salt}])/$ ($\text{mol}\cdot\text{kg}^{-1}$)	anion
−2765	−421	0.398	PO_4^{3-}
		0.459	$\text{C}_6\text{H}_5\text{O}_7^{3-}$
−1789	−272	0.554	HPO_4^{2-}
−1315	−245	0.538	CO_3^{2-}
−1295	−249	0.532	SO_3^{2-}
−1080	−200	0.524	SO_4^{2-}
−1090		0.501	$\text{C}_4\text{H}_4\text{O}_6^{2-}$
−465	−166	0.772	H_2PO_4^-
−430	−161	0.737	OH^-
−365	−170	0.978	CH_3CO_2^-
	−129	1.014	HSO_4^-
−335	−137	1.179	HCO_3^-
−340	−75	1.565	Cl^-
$\Delta_{\text{hyd}}G/$ ($\text{kJ}\cdot\text{mol}^{-1}$)	$\Delta_{\text{hyd}}S/$ ($\text{J}\cdot\text{K}^{-1}\cdot\text{mol}^{-1}$)	$([\text{IL}] = [\text{salt}])/$ ($\text{mol}\cdot\text{kg}^{-1}$)	cation (salt)
−1830	−331	0.792	Mg^{2+} ($\text{Mg}(\text{CH}_3\text{CO}_2)_2$)
		1.096	Mg^{2+} (MgCl_2)
−1505	−252	0.789	Ca^{2+} ($\text{Ca}(\text{CH}_3\text{CO}_2)_2$)
		1.252	Ca^{2+} (CaCl_2)
−1386	−242	1.148	Sr^{2+} (SrCl_2)
−1992	−351	1.095	Ni^{2+} (NiCl_2)
−365	−111	0.987	Na^+ (NaCH_3CO_2)
		1.565	Na^+ (NaCl)
−295	−74	1.206	K^+ (KCH_3CO_2)
		1.831	K^+ (KCl)
−258	−59	1.989	Cs^+ (CsCl)

For the salt anions, the plot of the saturation solubilities as a function of the Gibbs free energy of hydration is depicted in Figure 4. The results seem to indicate that the salting-out ability increases with the Gibbs free energy of hydration. Nevertheless, while for divalent anions the Gibbs free energy of hydration varies between -1000 and -2000 $\text{kJ}\cdot\text{mol}^{-1}$ and the saturation solubilities remain almost constant, the Gibbs free energy of

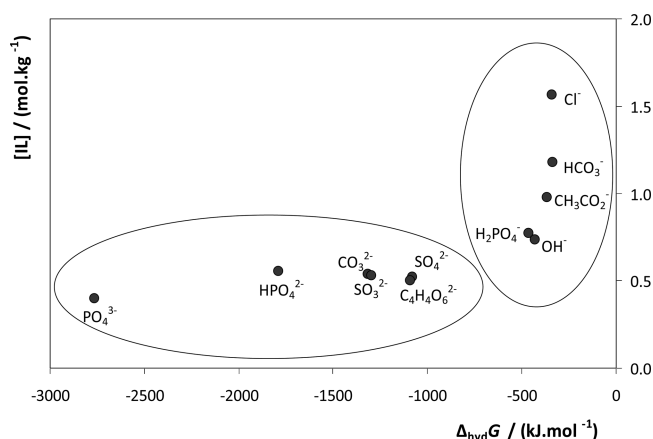


Figure 4. Relationship between the molality of ionic liquid necessary to undergo liquid–liquid demixing and the molar Gibbs free energy of hydration of the anions.

hydration for the monovalent ions varies in a narrower range (between -350 and -450 $\text{kJ}\cdot\text{mol}^{-1}$), and a large impact on their saturation solubilities is visible. However, when the molar entropy of hydration of the ions is further used to correlate the saturation solubilities, a more clear dependency is obtained, as shown in Figure 5. Moreover, for the cations, there is a close

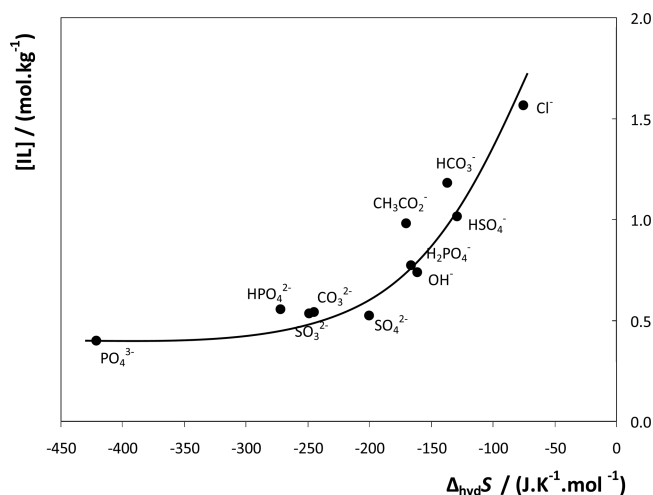


Figure 5. Relationship between the molality of ionic liquid necessary to undergo liquid–liquid demixing and the molar entropy of hydration of the anions.

relationship between the saturation solubilities and the molar entropy of hydration, observed for the two series of cations investigated, shown in Figure 6.

The results depicted in Figures 5 and 6 reveal that the strongest salting-out effect is achieved with the anions or cations of the salts with the highest values of molar entropy of hydration. This behavior confirms that, in agreement with results previously reported for hydrophobic ionic liquids,^{24–26} the salting-out of hydrophilic ionic liquids, such as $[\text{C}_4\text{mim}][\text{CF}_3\text{SO}_3]$, and thus the ABS formation, is majorly an entropically driven phenomenon. The interaction of the salt ions with water and the formation of their hydration complexes, which further cause the dehydration of the ionic liquid ions, rules the formation of ABSs involving ionic liquids.

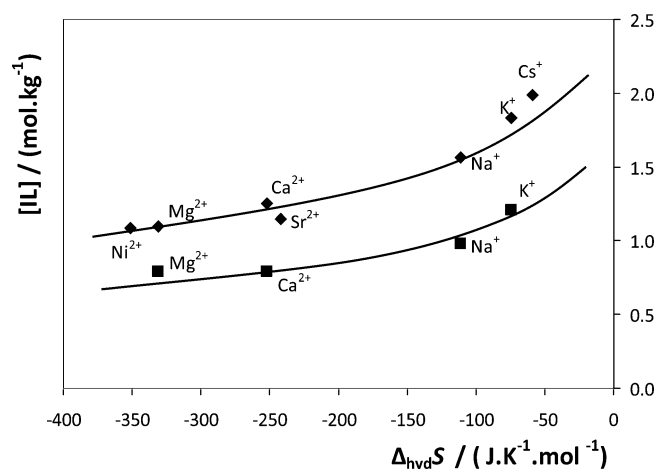


Figure 6. Relationship between the molality of ionic liquid necessary to undergo liquid–liquid demixing and the molar entropy of hydration of the cations: (◆) chloride-based salts, (■) acetate-based salts.

CONCLUSIONS

In this work, the ability of a broad range of salts, composed of diverse combinations of cations and anions, to induce the formation of $[\text{C}_4\text{mim}][\text{CF}_3\text{SO}_3]$ -based ABSs was evaluated. The respective ternary phase diagrams, TLs, and TLLs were determined at 298 K and atmospheric pressure. The large body of data obtained in this work shows that the ions' ability to induce the salting-out phenomenon follows the Hofmeister series and that the magnitude of the salting-out effect correlates with the molar entropy of hydration of the ions. The gathered results allowed us to conclude that the creation of ion–water complexes is the major driving force behind the formation of ionic-liquid-based ABSs.

ASSOCIATED CONTENT

Supporting Information

Experimental weight fraction data for the solubility curves. This material is available free of charge via the Internet at <http://pubs.acs.org>.

AUTHOR INFORMATION

Corresponding Author

*Tel: +351-234-370200. Fax: +351-234-370084. E-mail: jcoutinho@ua.pt

Notes

The authors declare no competing financial interest.

ACKNOWLEDGMENTS

This work was financed by national funding from FCT, *Fundação para a Ciência e a Tecnologia*, through the Projects PTDC/QUI-QUI/121520/2010 and Pest-C/CTM/LA0011/2011. The authors also acknowledge FCT for the postdoctoral and doctoral grants SFRH/BPD/41781/2007 and SFRH/BD/70641/2010 of M.G.F. and C.M.S.S.N., respectively.

REFERENCES

- (1) Shahriari, Sh.; Vossoughi, M.; Taghikhani, V.; Safekordi, A. A.; Alemzadeh, I. J. *Chem. Eng. Data* **2010**, *55*, 4968–4975.
- (2) Hatti-Kaul, R. *Aqueous Two-Phase Systems Methods and Protocols*; Humana Press: Totowa, NJ, 2000.
- (3) Albertson, P. A. *Partition of cell particles and macromolecules*; Wiley-Interscience, New York, 1986.

- (4) Madeira, P. P.; Reis, C. A.; Rodrigues, A. E.; Mikheeva, L. M.; Zaslavsky, B. Y. *J. Phys. Chem. B* **2010**, *114*, 457–462.
- (5) Gutowski, K. E.; Broker, G. A.; Willauer, H. D.; Huddleston, G. J.; Swatloski, R. P.; Holbrey, J. D.; Rogers, R. D. *J. Am. Chem. Soc.* **2003**, *125*, 6632–6633.
- (6) Abraham, M. H.; Zissimos, A. M.; Huddleston, J. G.; Swatloski, R. P.; Holbrey, J. D.; Rogers, R. D.; Acree, W. E., Jr. *Ind. Eng. Chem. Res.* **2003**, *42*, 413–418.
- (7) Najdanovic-Visak, V.; Canongia Lopes, J. N.; Visak, Z. P.; Trindade, J.; Rebelo, L. P. N. *Int. J. Mol. Sci.* **2007**, *8*, 736–748.
- (8) Wu, B.; Zhang, Y.; Wang, H. *J. Phys. Chem. B* **2008**, *112*, 6426–6429.
- (9) Shadeghi, R.; Golabiazar, R.; Shekaari, H. *J. Chem. Thermodyn.* **2010**, *42*, 441–453.
- (10) Sadeghi, R.; Mostafa, B.; Parsi, E.; Shahebrahimi, Y. *J. Phys. Chem. B* **2010**, *114*, 16528–16541.
- (11) Louros, C. L. S.; Cláudio, A. F. M.; Neves, C. M. S. S.; Freire, M. G.; Marrucho, I. M.; Pauly, J.; Coutinho, J. A. P. *Int. J. Mol. Sci.* **2010**, *11*, 1777–1791.
- (12) Cláudio, A. F. M.; Freire, M. G.; Freire, C. S. R.; Silvestre, A. J. D.; Coutinho, J. A. P. *Sep. Purif. Technol.* **2010**, *75*, 39–47.
- (13) Freire, M. G.; Neves, C. M. S. S.; Marrucho, I. M.; Canongia Lopes, J. N.; Rebelo, L. P. N.; Coutinho, J. A. P. *Green Chem.* **2010**, *12*, 1715–1718.
- (14) Pereira, J. F. B.; Lima, A. S.; Freire, M. G.; Coutinho, J. A. P. *Green Chem.* **2010**, *12*, 1661–1669.
- (15) Domínguez-Pérez, M.; Tomé, L. I. N.; Freire, M. G.; Marrucho, I. M.; Cabeza, O.; Coutinho, J. A. P. *Sep. Purif. Technol.* **2010**, *72*, 85–91.
- (16) Ventura, S. P. M.; Neves, C. M. S. S.; Freire, M. G.; Marrucho, I. M.; Oliveira, J.; Coutinho, J. A. P. *J. Phys. Chem. B* **2009**, *113*, 9304–9310.
- (17) Neves, C. M. S. S.; Ventura, S. P. M.; Freire, M. G.; Marrucho, I. M.; Coutinho, J. A. P. *J. Phys. Chem. B* **2009**, *113*, 5194–5199.
- (18) Cláudio, A. F. M.; Ferreira, A. M.; Shahriari, Sh.; Freire, M. G.; Coutinho, J. A. P. *J. Phys. Chem. B* **2011**, *115*, 11145–11153.
- (19) Bridges, N. J.; Gutowski, K. E.; Rogers, R. D. *Green Chem.* **2007**, *9*, 177–183.
- (20) Wang, Y.; Xu, X. H.; Yan, Y. S.; Han, J.; Zhang, Z. L. *Thermochim. Acta* **2010**, *501*, 112–118.
- (21) Li, S.; He, C.; Liu, H.; Li, K.; Liu, F. *J. Chromatogr., B* **2005**, *826*, 58–62.
- (22) Hofmeister, F. *Arch. Exp. Pathol. Pharmacol.* **1888**, *24*, 247–260.
- (23) Zhang, Y.; Cremer, P. S. *Curr. Opin. Chem. Biol.* **2006**, *10*, 658–663.
- (24) Freire, M. G.; Carvalho, P. J.; Silva, A. M. S.; Santos, L. M. N. B. F.; Coutinho, J. A. P. *J. Phys. Chem. B* **2009**, *113*, 202–211.
- (25) Freire, M. G.; Neves, C. M. S. S.; Silva, A. M. S.; Santos, L. M. N. B. F.; Marrucho, I. M.; Rebelo, L. P. N.; Shah, J. K.; Maginn, E. J.; Coutinho, J. A. P. *J. Phys. Chem. B* **2010**, *114*, 2004–2014.
- (26) Tomé, L. I. N.; Varanda, F. R.; Freire, M. G.; Marrucho, I. M.; Coutinho, J. A. P. *J. Phys. Chem. B* **2009**, *113*, 2815–2825.
- (27) Freire, M. G.; Louros, C. L. S.; Rebelo, L. P. N.; Coutinho, J. A. P. *Green Chem.* **2011**, *13*, 1536–1545.
- (28) Freire, M. G.; Neves, C. M. S. S.; Marrucho, I. M.; Coutinho, J. A. P.; Fernandes, A. M. *J. Phys. Chem. A* **2010**, *114*, 3744–3749.
- (29) Merchuk, J. C.; Andrews, B. A.; Asenjo, J. A. *J. Chromatogr., B* **1998**, *711*, 285–293.
- (30) Pegram, L. M.; Record, M. T., Jr. *J. Phys. Chem. B* **2008**, *112*, 9428–9436.
- (31) Collins, K. D.; Washbaugh, M. W. *Q. Rev. Biophys.* **1985**, *18*, 323–422.
- (32) Cacace, M. G.; Landau, E. M.; Ramsden, J. J. *Q. Rev. Biophys.* **1997**, *30*, 241–278.
- (33) Holz, M.; Grunder, R.; Sacco, A.; Meleleo, A. *J. Chem. Soc., Faraday Trans.* **1993**, *89*, 1215–1222.
- (34) Zhao, X.; Xie, X.; Yan, Y. *Thermochim. Acta* **2011**, *516*, 46–51.
- (35) Xie, X.; Han, J.; Wang, Y.; Yan, Y.; Yin, G.; Guan, W. *J. Chem. Eng. Data* **2010**, *55*, 4741–4745.
- (36) Zhao, X.; Xie, X.; Yan, Y. *Thermochim. Acta* **2011**, *516*, 46–51.
- (37) Amaresh, S. P.; Murugesan, S.; Regupathi, I.; Murugesan, T. *J. Chem. Eng. Data* **2008**, *53*, 1574–1578.
- (38) Zafarani-Moattar, M. T.; Zaferanloo, A. *J. Chem. Thermodyn.* **2009**, *41*, 864–871.
- (39) Johansson, H.; Karlström, G.; Tjerneld, F.; Haynes, C. A. *J. Chromatogr., B* **1998**, *711*, 3–17.
- (40) Ananthapadmanabhan, K. P.; Goddard, E. D. *J. Colloid Interface Sci.* **1986**, *113*, 294–296.
- (41) Rogers, R. D.; Bauer, C. B. *J. Chromatogr., B* **1996**, *680*, 237–241.
- (42) Zafarani-Moattar, M. T.; Hosseinpour-Hashemi, V. *J. Chem. Eng. Data* **2012**, *57*, 532–540.
- (43) Silva, L. H. M.; Loh, W. *J. Phys. Chem. B* **2000**, *104*, 10069–10073.
- (44) Marcus, Y. *Ion Properties*; Marcel Dekker, Inc.: New York, 1997.
- (45) Marcus, Y. *J. Chem. Soc., Faraday Trans.* **1991**, *87*, 2995–2999.
- (46) Zafarani-Moattar, M. T.; Zaferanloo, A. *J. Chem. Thermodyn.* **2009**, *41*, 864–871.